

DEVELOPMENT OF A TANDEM-ELECTROSTATIC-QUADRUPOLE FOR ACCELERATOR-BASED BORON NEUTRON CAPTURE THERAPY

A.J. Kreiner^{1,2,3}, H. Di Paolo^{1,2}, A.A. Burlon^{1,2}, J.M.Kesque¹, A.A. Valda^{1,2}, M.E. Debray^{1,2}, Y. Giboudot¹, P. Levinas¹, M. Fraiman¹, V.Romeo¹, H.R.Somacal^{1,2}, D.M. Minsky^{1,2}.

¹ *Departamento de Física, Comisión Nacional de Energía Atómica, Av. Gral. Paz 1499, San Martín, Buenos Aires, 1650, Argentina. kreiner@tandar.cnea.gov.ar*

² *Escuela de Ciencia y Tecnología, Universidad Nacional de San Martín, M. de Irigoyen 3100, (1650) San Martín, Argentina.*

³ *CONICET, Av.Rivadavia 1917, (1033) Buenos Aires, Argentina.*

There is a generalized perception that the availability of suitable particle accelerators installed in hospitals, as neutron sources, may be crucial for the advancement of Boron Neutron Capture Therapy (BNCT). An ongoing project to develop a Tandem-ElectroStatic-Quadrupole (TESQ) accelerator for Accelerator-Based (AB)-BNCT is described here. The project goal is a machine capable of delivering 30 mA of 2.5 MeV protons to be used in conjunction with a neutron production target based on the ${}^7\text{Li}(p,n){}^7\text{Be}$ reaction slightly beyond its resonance at 2.25 MeV. A folded tandem, with 1.25 MV terminal voltage, combined with an ESQ chain is being designed and constructed. This machine is conceptually shown to be capable of accelerating a 30 mA proton beam to 2.5 MeV. These are the specifications needed to produce sufficiently intense and clean epithermal neutron beams, based on the ${}^7\text{Li}(p,n){}^7\text{Be}$ reaction, to perform BNCT treatment for deep-seated tumors in less than an hour. This electrostatic machine is the technologically simplest and cheapest solution for optimized AB-BNCT. The first design and construction of an ESQ module is discussed and its electrostatic fields are investigated theoretically and experimentally. Also new beam transport calculations through the accelerator are presented.

I. INTRODUCTION

Boron Neutron Capture Therapy (BNCT) is considered by a significant international community as a promising option for the treatment of certain types of cancer.¹ While a great deal of progress has been made and will continue to be made using nuclear reactors, we are convinced that the advancement of BNCT will require neutron sources suitable for installation in hospital

environments. Low-energy particle accelerators are most appropriate for this purpose and can be constructed for modest cost, comparable to that of other medical devices.²⁻¹⁰ Furthermore, it is highly likely that the presence of these devices in specialized health-care institutions may be crucial for the future of BNCT in terms of a qualitative improvement in our ability to gather data and experience, patient recruitment, on-site resources and institutional commitment. A major advantage of Accelerator-Based BNCT (AB-BNCT) over reactor-based neutron sources is the potential for siting within a hospital. Accelerators offer a number of advantages over reactor-based sources for clinical applications: a) Accelerators can be easily turned off when the neutron field is no longer required. This, and the fact that neutrons are not produced via a critical assembly of fissile material, means that licensing and regulations associated with installing and maintaining the neutron source are substantially simplified. b) The capital expense of an AB-BNCT system is substantially lower than that associated with installation of a reactor system in or near a hospital. c) Accelerators have been a prominent feature of radiotherapy departments in hospitals for years and hence clinicians have a longstanding experience with such devices for patient irradiation. d) The neutron energy spectrum from certain nuclear reactions is much softer than the one coming from fission, which makes it easier to generate the "ideal" epithermal neutron spectrum (needed to treat a deep seated tumor), and hence the quality of the neutron field can be designed to significantly exceed the quality of the neutron field for reactor-based neutron sources.²⁻¹⁰ We report here on a Tandem-ElectroStatic-Quadrupole (TESQ¹⁰) for this purpose. The project goal is a machine capable of delivering 30 mA of 2.3-2.5 MeV protons to be used in

conjunction with a neutron production target made of Li metal or a refractory Li compound and based on the ${}^7\text{Li}(p,n){}^7\text{Be}$ reaction slightly beyond its 2.25 MeV resonance (this is the optimal reaction due to its large yield and soft neutron spectrum).

The technologically simplest and cheapest solution points to an electrostatic machine. Existing electrostatic accelerators, produce only a few mA of proton beam current limited by the column design (an important precursor has been the compact Tandem developed at LABA, MIT²). High current density, as implied by a size limited 30 mA proton beam, needs strong focusing in the transverse plane. In this regard ESQ's (Ref. 3) have a much stronger focusing capability than the aperture lenses used in conventional Tandem accelerators. A TESQ column can be designed using a lower longitudinal electric field gradient than a Pierce column in multi-MeV beam energy applications. Strong transverse fields due to the ESQ's will also suppress secondary electrons sideways through the electrodes hence preventing induced X-rays and minimizing the risk for electrical breakdown. In the present work a compact combination of an ESQ column with a Tandem in a folded geometry is discussed. This option would allow the ion source to be operated at ground potential and would require the generation of only 1.25 MV to reach the desired 2.5 MeV proton energy. Such a machine requires an H^- ion source and the transport of a high intensity beam through an appropriate stripper. In this paper we concentrate on the construction and on the theoretical, numerical and experimental characterization of the first prototype of a focusing and accelerating quadrupole module. Likewise new calculations of beam transport along the machine are presented.

II. MATERIALS AND METHODS

Measurements and simulations to define the performance parameters of an accelerator for AB-BNCT have been performed by several groups²⁻¹⁰. Within this frame, the ${}^7\text{Li}(p,n){}^7\text{Be}$ reaction, relatively close to its energy threshold, is the most promising due to its high neutron yield without a too hard neutron energy spectrum. This reaction was explored using a thick LiF target at the electrostatic tandem accelerator TANDAR (TANDem ARgentino) at CNEA's facilities in Buenos Aires. Two different experiments, both involving a water-filled head phantom, were performed as a testing ground for simulations⁹. These experimental results were subsequently compared with Monte Carlo simulations and used to validate the calculation tool in our laboratory. Extensive Monte Carlo simulations were performed to obtain an optimized neutron production and beam shaping assembly design and included a study of the optimal beam energy subject to healthy tissue dose and treatment time constraints. The conclusion relevant to this work was that

a proton beam of 20 mA at 2.3-2.5 MeV on pure Li is sufficiently intense. However, taking into account that Li-metal melts at 180 °C and in spite of the fact that the heat dissipation problem can be solved, we have decided to also explore refractory Li compounds of much higher melting point to minimize complications. The penalty in terms of yield for doing so is not too high for some compounds (like Li_2O). Hence our design goal has been taken at 30 mA (considering also a safety margin, the possibility of smaller irradiation times and/or smaller beam energies, etc).

In order to make a decision as to the most appropriate accelerator for BNCT, different options have been evaluated, such as d-d and d-t neutron generators, RFQ's and electrostatic machines of various types. The technologically simplest and cheapest solution points to an electrostatic machine. Most existing DC electrostatic accelerators can produce only a few mA of beam current, limited by the column design. For sufficiently high space-charge densities, as implied by a size limited multi-mA beam, particles carrying the same charge will repel each other, causing the ion beam to self-expand. Hence high beam current density needs strong transverse focusing. In conventional machines, thick apertures accomplish the beam focusing. In such arrangements the equipotential lines are periodically compressed and expanded, creating a series of alternating converging and diverging lenses, which provide net focusing. However, for such a cylindrical geometry, the radial focusing force is functionally coupled to the longitudinal acceleration force. Thus, the threshold of electrical breakdown along the beam axis limits beam focusing. In the paraxial approximation one has $E_r(r,z) = -(r/2)\partial E_z(0,z)/\partial z$ (Ref. 3, 13), which means that sufficiently strong transverse focusing means large longitudinal field gradient. A TESQ column can be more easily designed without exceeding the axial acceleration gradient limit. In fact an ESQ chain can provide much stronger transverse fields than the aperture lens by effectively decoupling the two functions: longitudinal acceleration in the gaps between the quadrupoles and transverse focusing within each quadrupole. The strong transverse field in an ESQ not only focuses the beam but also suppresses secondary electrons, and associated induced X-rays, preventing them from cascading downstream and minimizing the risk of electrical breakdowns. The alternating compression and decompression of the beam in successive quadrupoles in both x and y-axes of the ESQ chain produces a net beam focusing effect.

II.A. The theoretical electrostatic potential

The geometry in the center of the quadrupoles is shown in fig. 1 (horizontal section perpendicular to the longitudinal z axis). This arrangement has two discrete symmetries: a) the potential is invariant when the

azimuthal angle is increased in π , b) the potential changes sign when the angle is incremented in $\pi/2$.

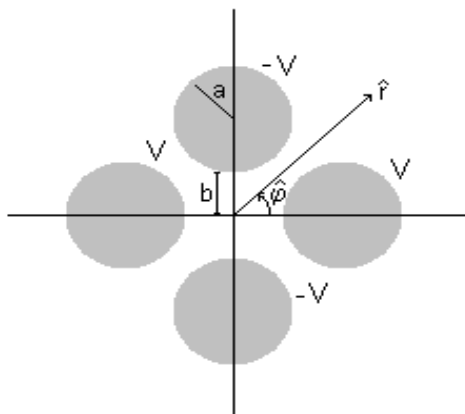


Fig. 1. Horizontal cross section in the center of a quadrupole.

When these two discrete symmetries are used the solution of the Laplace equation can be expressed as in eq. (1):

$$\Phi(r, \varphi)/V = a_0 + \sum_{n=1}^{\infty} a_n (r_n/b)^n \cos(n\varphi) \quad (1)$$

Where n is restricted to $2, 6, 10, 14, \dots, 2 + 4k$ ($k \geq 0$). For the potential choice of fig.1 the constant term is zero (if the potential on the positive poles would be $2V$ and the other 0 , the constant term a_0 would be equal to V).

It is highly desirable in order to transport the beam with minimal losses to have electric fields as linear as possible. This is achieved if the field is as quadrupolar as possible in the central portion of the device (along the z axis, within the circle of radius b). In order to achieve this condition the ratio a/b is varied until the coefficient of the dodecapole ($n=6$) term (a_6) vanishes.¹¹

Fig. 2 illustrates one possible method to implement this condition. Due to the symmetry of the problem it is sufficient to consider the values of the potential in the first half-quadrant (angles less than $\pi/4$). We have chosen 200 points on the quadrupole boundary (at potential V) and fitted the expansion in order to reproduce this condition, as a function of the ratio a/b , until the dodecapole term becomes very small.

In addition 2D and 3D finite element numerical calculations have been performed and good agreement is found between the two methods for the 2D problem (fig. 1).

II.B. The experimental electrostatic potential

The experimental electrostatic potential has been obtained using the electrolytic tank method¹². The prototype has been submerged in deionized water and the electrodes fed by an AC (about 1 kHz) low-voltage, high precision,

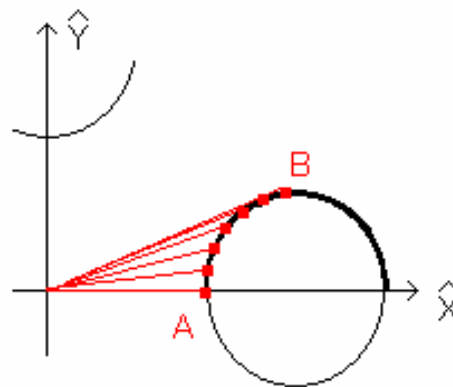


Fig. 2. Points on the contour of one of the quadrupoles (at potential V) used to determine the coefficients of the expansion of eq. (1).

pulse generator. AC is taken to avoid electrolysis products to build up at the electrodes which could distort the measurement. The voltage as a function of position within the central channel of the quadrupole has been measured with a precision voltmeter connected to a small 1 mm diameter silver sphere at the tip of a thin glass tube, mounted on an X, Y, Z home made stage (see fig. 4).

II.C. Transport calculations along the ESQ chain

The method used so far to calculate the transmission of the proton beam through the accelerator has been to solve the envelope equations¹³ taking into account the finite emittance with which the beam is born at the ion source and the self forces arising from space charge. We are presently investigating the best geometry of the quadrupoles (mainly length) and the width of the accelerating gaps. Sample calculations will be shown in the next section.

III. RESULTS AND DISCUSSION

Fig. 1 of Ref. 11 shows a general layout of the facility based on a folded Tandem and two electrostatic quadrupole chains within the acceleration tubes. It consists of a compact combination of an ESQ column with a Tandem in a folded geometry. This option allows the ion source to be operated at ground potential and requires the production of only 1.25 MV to reach the required 2.5 MeV proton energy.

Fig. 2 of Ref. 11 partially shows the ascending and descending quadrupole chains within the accelerator tubes, the 100 kV high-voltage units (switching type power supplies) operating in air and the low frequency generators driven by insulated shafts attached to motors, which in turn feed the 100 kV power supplies.

Fig. 3 shows a drawing (vertical cross section through central axis) of two focusing and accelerating

quadrupole modules with typical voltage values and dimensions in mm. The accelerating gap width of 250 mm, as the quadrupole length of 440 mm are just initial proposals. We are studying the optimum transfer through the accelerator as a function of these quantities. In fact, the accelerating gap will be most likely much smaller, of the order of 2 cm.

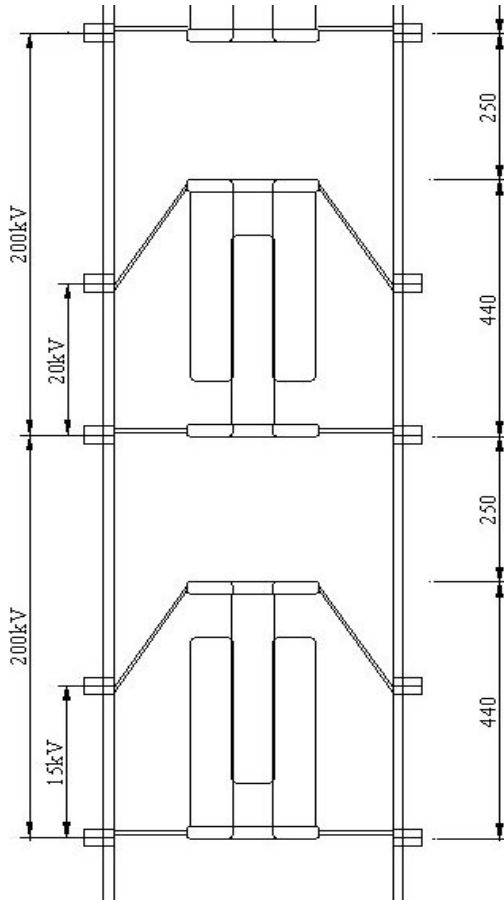


Fig. 3. Drawing of two consecutive focusing and accelerating quadrupole modules.

Fig. 4 shows a picture of our first focusing and accelerating quadrupole module with the XYZ stage on top to guide the voltage probe.

III.A. The theoretical electrostatic potential

The results for the coefficients of an expansion up to $n=14$, fitted to the potential calculated in 2D with the finite element method, are given in Table I and a_6 as a function of a/b is shown in Fig. 5.



Fig. 4. Picture of the quadrupole prototype with the focusing part (center), the accelerating gap (bottom) and the XYZ stage mounted on top.

The radius b has been taken as (30.0 ± 0.1) mm and for the potential we have taken $V = 1$ Volt (in other words we are fitting the potential relative to the V value). To secure a precision of a tenth of a millimeter in the geometrical dimensions we need to work with a precision of 1 in 1000 in the value of the a/b ratio. To this precision, the ratio which makes the coefficient of the dodecapole term vanish turns out to be 1.145 (the value given in the literature¹¹ is 1.146). The prototype has in fact been built with this specification. We are presently refining the mesh with the finite element code working both in 2 and 3

TABLE I. Coefficients of the multipolar expansion of eq. (1) for $a/b=1.145$.
(2)

| nth coefficient | Value (for $V=1V$) (error) |
|-----------------|-----------------------------|
| a_2 | 1.00281 (4E-6) |
| a_6 | 0.000032 (4E-6) |
| a_{10} | 0.00235 (3E-6) |
| a_{14} | 0.00024 (7E-7) |

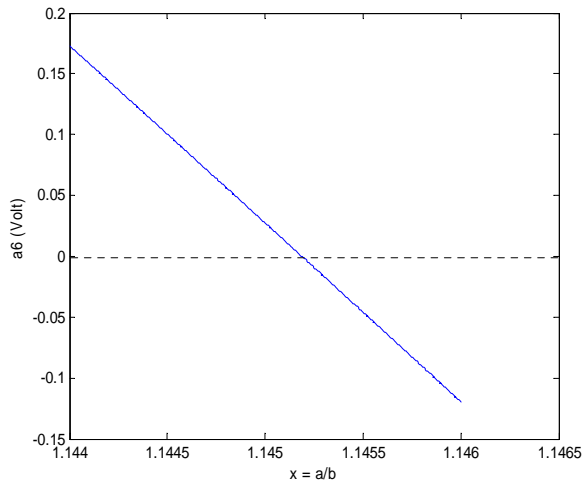


Fig. 5. Coefficient a_6 of the dodecapole term as a function of the a/b ratio.

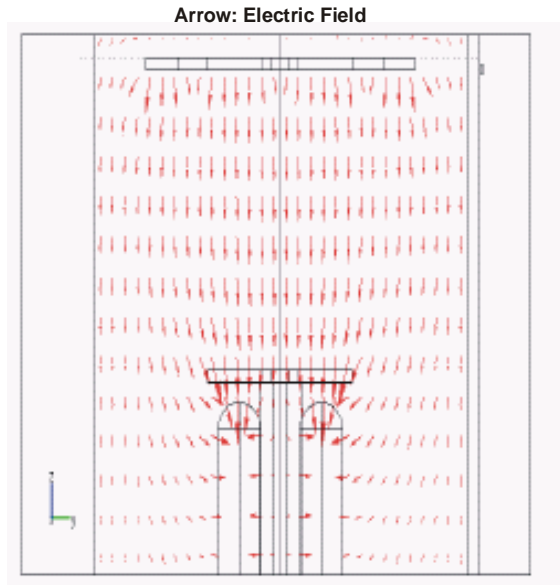


Fig. 6. Electric field vectors in the vertical midplane of the quadrupole module.

dimensions to consolidate this figure. Fig. 6 shows a vertical central section in which the electric field is calculated. The field in the gap is essentially longitudinal while within the quadrupole it is predominantly transverse.

III.B. The experimental electrostatic potential

Some sample measurements of the experimentally obtained electrostatic potential are shown in fig. 7, 8 and 9. Fig. 7 gives the ratio of the potential measured by the spherical silver probe (V_{sonda}) to the applied source

potential (V_{Fuente}) as a function of the azimuth angle and for fixed $r = 24$ mm.

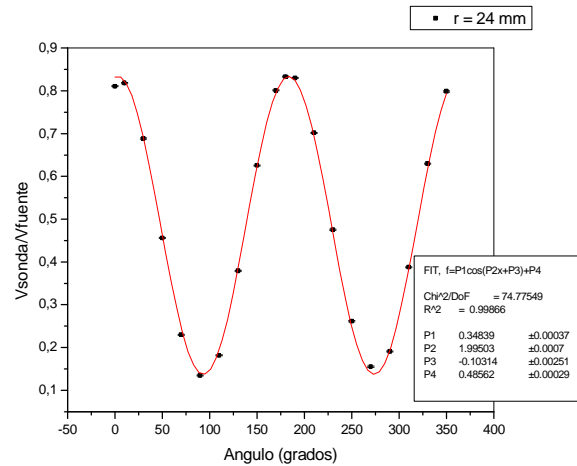


Fig. 7. Measured voltage ratio as a function of angle for fixed radius $r = 24$ mm.

Fig. 8 gives the relative potential (V_s/V_f) as a function of the distance to the axis (in the center plane of the quadrupole) for a number of different angles. Both figs. 7 and 8 correspond to the center plane of the quadrupole.

$$\Phi(r, \varphi) = a_0 + \sum_{n=1}^{\infty} a_n (r_n / a)^n \cos(n\varphi) \quad (2)$$

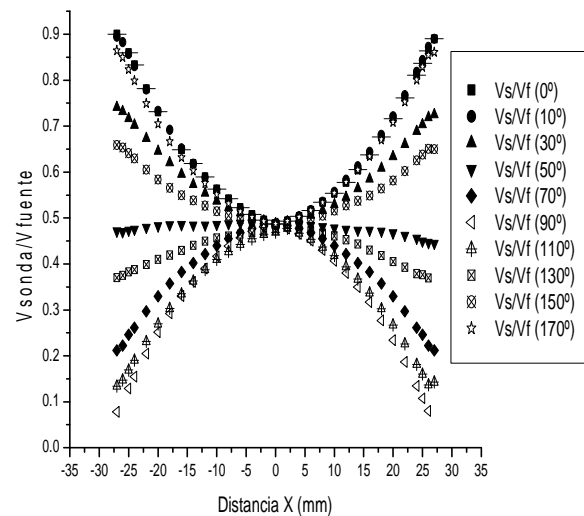


Fig. 8. Measured voltage ratio as a function of radius for a number of fixed angles (e.g., 0° corresponds to the direction between the two positive poles).

This set of data has been fitted with the help of eq. (2). In this fit we have included all terms up to $n=6$ ($n=1,2,3,4,5,6$), in order to allow for possible asymmetries. Table II shows the results. It should be noted that here the potential of the two negative poles was taken as ground ($V=0$), which is the reason for an a_0 near 0.5. All the coefficients with n larger than 2 are very small, in fact $n=3, 5$ are compatible with zero within errors. The other terms a_4 and a_6 are also almost zero within errors.

TABLE II. Fitted coefficients of the multipole expansion (2) for the experimental module.

| Coefficient | Fitted value (mV/mm ²) |
|-------------|------------------------------------|
| a_0 | 0.483 ± 0.002 |
| a_2 | 0.540 ± 0.005 |
| a_3 | 0.000 ± 0.007 |
| a_4 | 0.013 ± 0.009 |
| a_5 | 0.002 ± 0.009 |
| a_6 | -0.016 ± 0.009 |

Finally fig. 9 shows the potential along the vertical axis of the quadrupole ($z=0$ is the center). The potential is quite constant within the device reaching $\pm V$ at the ends.

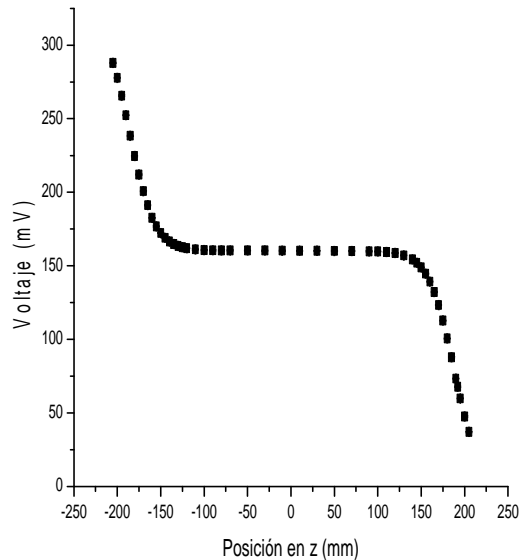


Fig. 9. Measured voltage as a function of the vertical position z along the axis of the quadrupole.

III.C. Transport calculations along the ESQ chain

Fig. 10 shows the beam envelopes for the vertical and horizontal planes containing the propagation axis (Z) for the upgoing chain of q-poles from the ion source to the high voltage terminal, where the beam reaches 1.25 MeV.

These beam envelopes for a 30 mA proton beam have been calculated including (1) a finite normalized invariant emittance¹³ of $\pi\epsilon_n = \beta\gamma\pi\epsilon = \beta\gamma \iint dx dx' = 0.253 \pi \cdot \text{mm} \cdot \text{mrad}$ on both YZ and XZ planes and (2) space charge effects (ϵ_n corresponds to 4 times the true rms emittance to reproduce the emittance value of a K-V distribution; β and γ are the usual relativistic magnitudes for the accelerated particle). 12 quadrupoles (6 q-pole accel-decel modules) have been used: all 30 cm long and with a bore hole radius of 3 cm and 2 cm wide accelerating gaps between them. The voltages between the opposite polarity Y and X poles are: 4.75, 5.65; 6.25, 6.78; 7.20, 7.43; 7.73, 7.99; 8.23, 8.45 and 8.65, 8.84 kV respectively. These calculations show that it is possible to guide a 30 mA beam confined to a radius smaller than about 13 mm through the accelerator.

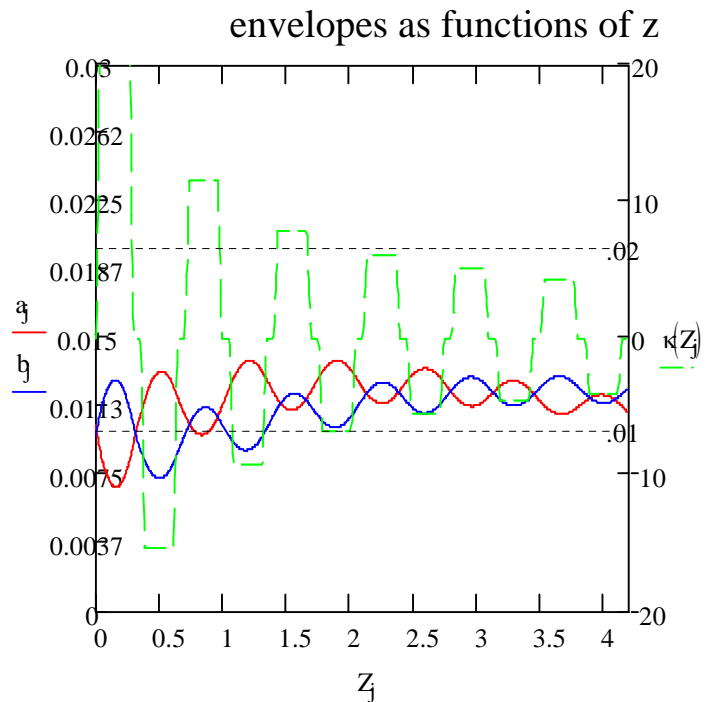


Fig. 10. Envelopes $a(z)$ (xz plane) and $b(z)$ (yz plane) as functions of z in meters (the total length of the upgoing q-pole chain is about 4 m). The left-hand side vertical scale is also in m (3 cm corresponds to the radius of the circle inscribed into the 4 poles). The maximum beam excursion in both directions is seen to be 1.2 to 1.3 cm. The right-hand side vertical scale pertains to the magnitude κ , the coefficient in the envelope equations related to the strength of the quadrupole field.¹³

IV. CONCLUSIONS

High proton-current (20-30 mA) machines are necessary for hospital based AB-BNCT. This high current requires strong transverse focusing and hence the proposal to use an ESQ. A folded Tandem requires a

terminal voltage of only 1.25 MV and less space. It allows ion source operation outside of the machine at ground potential. Electrostatic technology is most appropriate for its low cost and simplicity.

A first prototype of a focusing-accelerating quadrupole module has been constructed and its electrostatic field calculated and measured. The emphasis has been set in the determination of the optimal ratio between the radius of the central region in which the beam circulates and the radius of the cylindrical quadrupoles, in order to find the precise value for which the dodecapole term vanishes. Extensive beam envelope calculations have been performed in order to explore the best geometry for keeping the beam as close as possible to the central axis of the device. More systematic searches for the optimal configuration are in progress.

ACKNOWLEDGMENTS

Financial support from ANPCYT is kindly acknowledged.

REFERENCES

1. J. CODERRE et al., *Appl. Rad. and Isot.* **61**, (2004)5.
2. J.C. YANCH, X-I. ZHOU, R.E. SHEFER, R.E. KLINKOWSTEIN, "Accelerator-based epithermal neutron beam design for NCT", *Med. Phys.* **19**, pp.709-721 (1992) and references therein.
3. J. W. KWAN, E. HENESTROZA, C. PETERS, L.L. REGINATO, AND S.S. YU, "Designs of a DC ESQ Accelerator for BNCT Application", *Application of Accelerators in Research and Industry*, AIP Press, pp.1313-1315 (1997) and references therein.
4. F.WHEELER, D.NIGG, J. CAPALA, P.WATKINS, C.VROEGINDEWEIJ, I.AUTERINEN, T.SEPPALA AND D.BLEUEL, *Med. Phys.* **26(7)**, 1237 (1997).
5. B.F.BAYANOV et al., "Accelerator-based neutron source for the neutron-capture and fast neutron therapy at hospital", *Nuclear Instruments & Methods in Physics Research*, **A413**, 397(1998).
6. D.L.BLEUEL, R.J.DONAHUE, B.A.LUDEWIGT, J.VUJIC, "Designing accelerator-based epithermal neutron beams for BNCT", *Med.Phys.***25**, pp.1725-1734 (1998).
7. K.TANAKA, T.KOBAYASHI, Y.SAKURAI, Y.NAKAGAWA, M.ISHIKAWA, M.HOSHI", "Irradiation characteristics of BNCT using near-threshold ${}^7\text{Li}(p,n)$ direct neutrons, application to intraoperative BNCT for malignant brain tumors", *Phys.Med.Biol.***47**, pp.3011-3032 (2002) and references therein.
8. T.E.BLUE AND J.C.YANCH, *Journal of Neuro-Oncology* **62(1)**, 19 (2003) and references therein.
9. A.A.BURLON, A.J.KREINER, A.A.VALDA, D.M.MINSKY, H.R.SOMACAL, M.E.DEBRAY, AND P.STOLIAR, "Optimization of a neutron production target and a beam shaping assembly based on the ${}^7\text{Li}(p,n)$ reaction for BNCT", *Nucl. Instr. and Meth. in Phys. Res.* **B229/1**, 144-156 (2005).
10. A.J. KREINER, J.W. KWAN, A.A. BURLON, H. DI PAOLO, E. HENESTROZA, D.M. MINSKY, A.A.VALDA, M.E. DEBRAY, AND H.R. SOMACAL, "A Tandem-electrostatic-quadrupole for accelerator-based BNCT", *Nuclear Instruments and Methods in Physics Research B* 261 (2007) 751-754.
11. S. OKAYAMA, H. KAWAKATSU, *J Phys B: Sci. Instrum.* Vol 11, 211 (1978).
12. J.C.FRANCKEN in *Focusing of Charged Particles*, pp.101, Ed. A. Septier, Vol.I, Academic Press (1967).
13. J. D. LAWSON, *The Physics of Charged-Particle Beams*, pp.158, Clarendon Press, Oxford, 1988.